BEVA2.0: Modular Assembly of Golden Gate-Compatible Vectors with Expanded Utility for Genetic Engineering

Barney A. Geddes[a]*, Riley Williamson[a], Jake Schumacher[a], Ahmad Ardi[a], Garrett Levin[a], Emily Červenka[b], Rui Huang[b] and George C. diCenzo[b]

[a] Department of Microbiological Sciences, North Dakota State University, Fargo, ND, USA.
[b] Department of Biology, Queen's University, Kingston, ON, Canada.

* Corresponding Author: Barney Geddes, barney.geddes@ndsu.edu

Abstract

This expansion for the modular vector assembly platform BEVA (Bacterial Expression Vector Archive) introduces 11 new BEVA parts including two new cloning site variants, two new antibiotic resistance modules, three new origins of replication, and four new accessary modules. As a result, the modular system is now doubled in size and expanded in its capacity to produce diverse replicating plasmids. Furthermore, it is now amenable to genetic engineering methods involving genome-manipulation of target strains through deletions or integrations. In addition to introducing the new modules, we provide several BEVA-derived Golden Gate cloning plasmids that are used to validate parts and that may be useful for genetic engineering of proteobacteria and other bacteria. We also introduce new parts to allow compatibility with the CIDAR MoClo parts libraries.

Keywords

Synthetic biology, Golden Gate cloning, Genetic engineering, Plasmid

Introduction

Since its inception, Golden Gate DNA assembly technology has revolutionized the ability to rapidly assemble multiple fragments of DNA in linear orders, facilitating advancements in synthetic biology (Engler *et al.*, 2009). This technique, particularly through the MoClo (Modular Cloning) system, has enabled the hierarchical assembly of genetic constructs using standardized parts, making it a powerful tool for researchers. MoClo's early adoption was largely driven by plant science research, where it was used to develop constructs for plant engineering via *Agrobacterium* tDNA integration (Werner *et al.*, 2012). This led to the creation of extensive parts libraries and kits for plant engineering, such as those available through Addgene, which include promoters, untranslated regions, antigen tags, subcellular localization signals, marker genes, and terminators (Weber *et al.*, 2011; Werner *et al.*, 2012; Engler *et al.*, 2014; Gantner *et al.*, 2018), as well as tools for genome editing (Hahn *et al.*, 2020; Grützner *et al.*, 2021; Stuttmann *et al.*, 2021). These resources have significantly accelerated synthetic biology by allowing researchers to rapidly assemble complex constructs using standardized parts.

While initially focused on plant engineering, the MoClo system naturally expanded to other organisms, including microorganisms. For example, parts kits have been developed for yeast hierarchical assembly (Lee *et al.*, 2015) and protein expression (Obst, Lu and Sieber, 2017), and the CIDAR MoClo Library was developed for bacteria (Iverson *et al.*, 2016), which includes a variety of useful synthetic biology parts sourced from the iGEM Registry of Standard Biological Parts. A CIDAR MoClo Expansion was also released that includes even more promoters, ribosome binding sites, coding sequences, and terminators, further enhancing its utility in synthetic biology. Useful systems for protein expression in *Escherichia coli* have also been developed (Moore *et al.*, 2016; Bentham *et al.*, 2021). However, with the widespread adoption of Golden Gate cloning, and new parts libraries in research labs around the world, there has been a growing need for new Golden Gate-compatible vectors with utility in a wide variety of organisms. To address this, we previously developed the Bacterial Expression Vector Archive (BEVA), a system that enables the assembly of Golden Gate cloning vectors from a library of standardized parts using a MoClo-like hierarchical assembly approach (Geddes, Mendoza-Suárez and Poole, 2019).

The field of microbial engineering continually seeks more efficient and versatile methods for designing plasmids to deliver and express genetic cargo. BEVA and the Standard European

58 Vector Architecture (SEVA) (Silva-Rocha *et al.*, 2013), which was recently adapted for Golden
59 Gate cloning (Martínez-García *et al.*, 2023), have emerged as promising tools due to their
60 modular approach and ease of vector design, offering a path toward high-throughput
61 applications. These models streamline the process of assembling complex genetic constructs by
62 providing standardized, interchangeable modules that can be easily arranged in various
63 configurations.
64 In this work, we report the creation of 11 new modules that significantly expand the
65 utility of BEVA. We also generate and validate the performance of several new Golden Gate
66 vectors that utilize the modules. The new vectors expand the utility of BEVA in two ways. First,
67 they increase the capacity to generate useful expression vectors for diverse bacterial taxa by
68 incorporating additional antibiotic resistance genes and broad host range origins of replication.
69 Second, they incorporate modules that allow the generation of vectors useful for bacterial
70 genome engineering, either through homologous or site-specific recombination. Overall, this
71 study not only expands the BEVA toolkit but also contributes to the broader goal of developing
72 versatile and efficient plasmid systems for microbial engineering.
73
74 **Materials and Methods**
75 **Design of new BEVA modules**
76 New BEVA modules were designed based on functional units from pre-existing cloning vectors
77 and synthesized free of internal BsaI, BpiI (BbsI) and BsmBI (Esp3I) sites by Twist Bioscience
78 in the Amp^R backbone "pTwist Amp High Copy", Cm^R backbone "pTwist Chlor High Copy, or
79 cloned via BsaI into Cm^R pGGAselect (New England Biolabs). In some cases, prototypes were
80 designed by PCR amplification and cloning into pJet1.2, with the resulting vectors then used for
81 generating Level 1 cloning vectors (pQGG002-005). However, these modules were later
82 recloned into pGGAselect or resynthesized in the pTwist Chlor/Amp High Copy plasmids to
83 eliminate a BsaI site from the pJet1.2 backbone that caused cloning efficiency issues.
84
85 *Golden Gate cloning sites*
86 Two new Level 1 cloning site modules were generated by altering the Level 1 cloning site from
87 pOGG004. For pNDGG021 and pNDGG022, we excluded the T0 terminator 3' of the cloning
88 site. For pNDGG022, we further altered the 5' BsmB1(Esp31) fusion site to CAGA to allow by-

89 passing of the endlinker/terminator modules that include the *rrnB* T1 terminator and to allow for
90 directly connecting these modules to a Position 4 module 3' fusion site, thus completely
91 excluding terminators flanking Level 1 cloning sites.
92
93 *Antibiotic resistance cassettes*
94 Antibiotic resistance modules were flanked by 5' BsmB1(Esp31)-GCAA and 3' ACTA-
95 BsmB1(Esp31) sites to enable cloning as Position 2 modules in BEVA. For the
96 kanamycin/neomycin resistance gene *nptII* (in pNDGG001), we used 1,036 bp from the cloning
97 vector pTH1937 (Milunovic *et al.*, 2014) that included the *nptII* open reading frame and 241 bp
98 upstream which was cloned into pGGAselect via BsaI. For the spectinomycin resistance gene
99 *aadA* (in pNDGG002), we synthesized 1,786 bp from the pHP45Ωspec interposon (Prentki and
100 Krisch, 1984) that contained the *aadA* open reading frame with 516 upstream and 259 bp
101 downstream regions in pTwist Amp High Copy.
102
103 *Origins of replication and transfer*
104 Three new origins of replication and transfer were generated. These modules were each flanked
105 by 5' BsmB1(Esp31)-ACTA and 3' TTAC-BsmB1(Esp31) sites to enable cloning as Position 3
106 modules in BEVA. The sequences of the origins p15A (pNDGG006) and pMB1 (pNDGG007),
107 including their *oriT*s, were derived from 1,492 bp and 980 bp segments from pTH1937
108 (Milunovic *et al.*, 2014) and pUCP30T (Schweizer and Hoang, 1996), respectively. pMB1 was
109 cloned into pGGAselect via BsaI, while p15A was synthesized in pTwist Chlor High Copy. The
110 broad host range origin RSF1010 (3,078 bp) was PCR amplified from pRSF-LtetO-GFP (Lee *et*
111 *al.*, 2019) and combined with a 268 bp *oriT* amplified from pOGG026 (Geddes, Mendoza-Suárez
112 and Poole, 2019) by BsaI Golden Gate cloning into pGGAselect to generate pNDGG005.
113
114 *Accessory modules*
115 Four accessory modules were added, each flanked with 5' BsmB1(Esp31)-TTAC and 3' CAGA-
116 BsmB1(Esp31) sites to enable cloning as Position 4 modules in BEVA. The *sacB* gene enabling
117 sucrose counterselection was designed based off of pJQ200SK (Quandt and Hynes, 1993), and
118 the resulting module in pNDGG008 included 1,944 bp surrounding the *sacB* open reading frame
119 including 446 bp upstream and 76 bp downstream.

120 The *FRT* site-specific Flp recombinase motif
121 (GAAGTTCCTATTCCGAAGTTCCTATTCTCTAGAAAGTATAGGAACTTC) was
122 synthesized as a Position 4 module in pNDGG009 with a few extra flanking base pairs to bring
123 the total size to 63 bp. The *attP* ϕC31 integrase target site
124 (CCCCAACTGGGGTAACCTTTGAGTTCTCTCAGTTGGGGG) was similarly synthesized as
125 a Position 4 module in pNDGG010. An *attP* motif was also included in pNDGG009 flanked by
126 BsaI (5'GCTT and 3'CGCT) sites (CIDAR EF module) such that it could be added to the 3' end
127 of an open reading frame in a Level 1 cloning. Likewise, a *FRT* motif flanked by the same BsaI
128 sites (5'GCTT/3'CGCT) was added to pNDGG010.
129 The I-SceI site accessary module in pQGG001 was generated by ligating the I-SceI site
130 as an annealed double-stranded oligomer (5' –
131 TCTGGACTACGGTTCCAAATTACCCTGTTATCCCTACCTTGGAATGGTCA - 3' and 5'-
132 TTACTGACCATTCCAAGGTAGGGATAACAGGGTAATTTGGAACCGTAGTC - 3') into
133 an *Esp3I*-digested pOGG012 backbone using T4 DNA ligase.
134
135 *CIDAR terminators*
136 Three terminators from CIDAR (T2m, T12m and T15m from CIDAR MoClo Extension Volume
137 I) were adapted such that the 3' fusion site matched BEVA L1 cloning vectors. The fusion site
138 was adapted during cloning as a Level 0 part into pOGG006. The same forward primer was used
139 for all three, which bound upstream of the 5' BsaI site and added a BpiI fusion site (TGCC) for
140 cloning into pOGG006 (5'- AAAGAAGACAATGCCCGGCCGCTTCTAGAGA-3'). A unique
141 3' primer was used for each, with the binding site anchored in the terminator and an altered 3'
142 BsaI fusion site added in the primer along with a BpiI fusion site for cloning into pOGG006
143 (T2m = 5'-AAAGAAGACAATCCCGGTCTCAAGCGTCTCAAGGGCGCAATAAAA-3';
144 T12m = 5'-AAAGAAGACAATCCCGGTCTCAAGCGTTGAGAAGAGAAAAGAAAACCG-
145 3', T15m = 5'-AAAGAAGACAATCCCGGTCTCAAGCGGGCAGACCAGAAACAAA-3'.
146 After cloning into pOGG006, the resulting plasmids functioned as Level 0 parts, for BEVA,
147 flanked by *BsaI* and the fusion sites GCTT (5') and CGCT (3').
148
149 **Golden Gate cloning**

150 Golden Gate cloning reactions were performed using forty fmol of plasmid parts in a reaction
151 mix recipe of 1 µl restriction enzyme (BsmBI-v2, Esp3I, or BsaI-HF-v2) (New England
152 Biolabs), 1.5 µl bovine serum albumin, 1 µl T4 DNA ligase (400 units/µL; New England
153 Biolabs), and 1.5 µl 10x T4 DNA ligase buffer, diluted with ddH_2O to a total volume of 15 µl.
154 Alternatively, NEB Golden Gate Assembly Kits (BsaI-HF-v2 or BsmBI-v2) were used as a pre-
155 mixed reaction mix with the DNA parts and ddH_2O. The Golden Gate cloning reactions were
156 performed in a thermocycler as follows: For BbsI/Esp3I: 30 cycles of 42°C for 1 minute
157 followed by 16°C for 1 minute, with heat inactivation at 60°C for 5 minutes; for BsaI: 30 cycles
158 of 37°C for 1 minutes and 16°C for 1 minute, with heat inactivation at 60°C for 5 minutes. The
159 resulting reaction mixes were stored at -20ºC before thawing and using to transform chemically
160 competent *E. coli* DH5α. Successful transformants were selected using appropriate antibiotics
161 and X-gal (5-bromo-4-chloro-3-indolyl-β-D-galactopyranoside). Successful vector constructions
162 were selected based on blue-colored colonies, while successful Level 1 clonings were selected
163 based on white-colored colonies. Plasmids were verified by diagnostic restriction digest and/or
164 whole plasmid long-read sequencing by Plasmidsaurus.
165
166 **Genetic manipulations**
167 Bacterial strains used in this work are listed in Table 1. *E. coli* and *Sinorhizobium meliloti* strains
168 were grown in liquid or solid Lysogeny Broth (LB) medium, supplemented with 0.25 mM
169 $MgCl2_2$ and 0.25 mM $CaCl_2$ (termed LBmc) for *S. meliloti. E. coli* strains were grown at 37°C
170 while *S. meliloti* strains were grown at 28°C. Antibiotics were added to media when necessary
171 for *E coli* (Ec) or *S. meliloti* (Sm), at the following concentrations: gentamicin 10 µg/ml (Ec) or
172 60 µg/ml (Sm), kanamycin 25 µg/ml (Ec), neomycin 200 µg/ml (Sm), spectinomycin 50 µg/ml
173 (Ec) or 100 µg/ml (Sm), ampicillin 100 µg/ml (Ec), and tetracycline 5 µg/ml (Ec or Sm). Sucrose
174 counterselection was performed by adding 10% sucrose to LB medium. Conjugations between *E.*
175 *coli* and *S. meliloti* were performed by triparental mating using *E. coli* MT616 as a helper strain
176 (Finan *et al.*, 1986). Tests for colony antibiotic resistance/sensitivity phenotypes were performed
177 by patching colonies onto replicated agar plates using a sterilized toothpick. Transformation into
178 *E. coli* and conjugation into *S. meliloti* by triparental mating were performed using routine
179 protocols (Finan *et al.*, 1986; Geddes, Mendoza-Suárez and Poole, 2019).
180

181 **Fluorescence measurements by flow cytometry and plate reader assays**
182 Preparation of cells for flow cytometry experiments were conducted as follows. Cells were
183 grown in LB media containing standard working concentrations of the antibiotic corresponding
184 to the plasmid-encoded resistance. Media was inoculated with a single colony and placed on a
185 shake incubator set to 37°C at 215 rpm and grown overnight. One ml of each cell culture was
186 transferred to individual 1.5 ml microtubes, after which their optical density was measured using
187 a spectrophotometer. The tubes were then centrifuged for one minute at 17,000 x g. The
188 supernatant was removed, and the pellet was resuspended in PBS (phosphate-buffered saline) to
189 a final OD600 (optical density at 600 nm) of 1.0. Resuspended cells were further diluted 1:100 in
190 PBS immediately prior to flow cytometry. Tubes containing the diluted samples were placed in
191 the flow cytometer receptacle one at a time. The Beckman Cytoflex S flow cytometer was set to
192 interrogate the cells using yellow and blue lights. The yellow light detectors were set to measure
193 an mScarlet-I band path of 585/42, and the blue light detectors were set to measure both GFP at
194 525/40 and SSC at 488/8. Speed settings were adjusted to reach an average of 1000 events per
195 second. These settings were adjusted depending on each sample but were generally kept at the
196 lowest speed of 10 µl/min. Samples were manually compensated when required.
197 For measurements of fluorescence by plate reader, a Cytation 5 was used to quantify
198 fluorescence across a bacterial growth curve. *E. coli* or *S. meliloti* were grown at 37ºC and 28ºC,
199 respectively, for 24 hours from a starting OD600 of 0.05. The OD600 and fluorescence was
200 measured every 20 minutes. The growth was analyzed using the Growthcurver package in R. The
201 fluorescent values presented are derived from the maximum doubling time in the growth curve.
202 The following parameters were used for fluorescent measurements: cfCFP - excitation 485,
203 emission 475, gain 90; sfGFP - excitation 485, emission 510, gain 60; sfYFP - excitation 510,
204 emission 535, gain 100; mScarlet-I - excitation 569, emission 593, gain 108.
205
206 **Results and Discussion**
207 **Expansion of BEVA with 11 new modules.**
208 We aimed to improve the utility of BEVA for the construction of useful Golden Gate vectors by
209 (1) expanding the potential host range with additional broad host range origin of replication and
210 antibiotic resistance modules, and (2) expand the utility to routinely used vectors for genome
211 manipulations (deletions/integrations) via the addition of narrow host range origins of

212 replication, counters-electable markers, and site-specific recombinase sites. To enable this, we
213 designed 11 new modules that are shown as part of the broader BEVA archive in **Figure 1** and
214 listed in **Table 1**. The rational for inclusion of each of the modules is described below.
215 The initial BEVA was largely designed as a platform for generating expression vectors
216 and hence included the broad host range origins of replication pBBR1 and RK2 with several
217 options for antibiotic resistance genes that could be tailored to a target strain of interest. To
218 facilitate wider host utility, we added another widely-used broad host range origin of replication,
219 RSF1010 (vector pNDGG005), as a Position 3 module. We also expanded available antibiotic
220 selection by adding spectinomycin resistance via *aadA* as a Position 2 module (vector
221 pNDGG002). While a kanamycin/neomycin resistance module (*aphA*-based) was available in the
222 original BEVA, we and others have found this module to be ineffective for neomycin-based
223 selection in *Sinorhizobium meliloti* (personal communication). Therefore, a new
224 kanamycin/neomycin module was added based on the more widely used *nptII* gene (vector
225 pNDGG001).
226 Genome manipulations in model bacteria such as *S. meliloti* 1021 routinely involve the
227 use of integrative, or "suicide", plasmids that replicate readily in *E. coli* but must integrate into
228 the genome to be maintained in the target microbe (Quandt and Hynes, 1993; diCenzo *et al.*,
229 2019). Integrations can be catalyzed by cloning a short sequence of the target genome to
230 facilitate integration at a specific genomic locus via homologous recombination. Double
231 homologous recombination can generate deletions in a similar approach by including target-
232 genome sites flanking a region to be deleted and incorporating a counter-selectable marker in the
233 vector backbone to catalyze its excision. An alternative to homologous recombination is to
234 utilize site-specific recombinases to catalyze integration at a target site in the host genome with a
235 compatible recombinase target sequence of an integrative plasmid (diCenzo and Finan, 2018).
236 These approaches can also be combined to catalyze inversions or large deletions between two
237 recombinase sites, following their integration on either side of a target region via two
238 heterologous integrative vector backbones. To facilitate all of these approaches, we added two
239 narrow host range origins (p15A and pMB1, vectors pNDGG006-7), two site-specific
240 recombinase sites (*FRT* and *attP*, vectors pNDGG009-10), and two counter-selectable markers
241 (I-SceI and *sacB*, vectors pQGG001 and pNDGG008, respectively). The I-SceI target sequence
242 can be counter-selected through expression of the I-SceI restriction enzyme from an introduced

plasmid (Aubert, Hamad and Valvano, 2014), while *sacB* can be counter-selected via sucrose toxicity (Quandt and Hynes, 1993). The *FRT* and *attP* sites facilitate recombination with *FRT* and *attP* sites via Flp recombinase and ϕC31 integrase, respectively (diCenzo and Finan, 2018). The availability of two heterologous narrow host range origins facilitates introductions of multiple plasmids by homologous recombination (such as for *FRT*-mediated deletions), minimizing the chance for recombination between them (diCenzo and Finan, 2018). To allow further minimization of homology between assembled plasmids, we also introduced three alternate Level 1 cloning sites (pNDGG021-23) that allow exclusion of the 3' T0 terminator or the 5' T1 terminator (via skipping an endlinker) from assembled vectors.

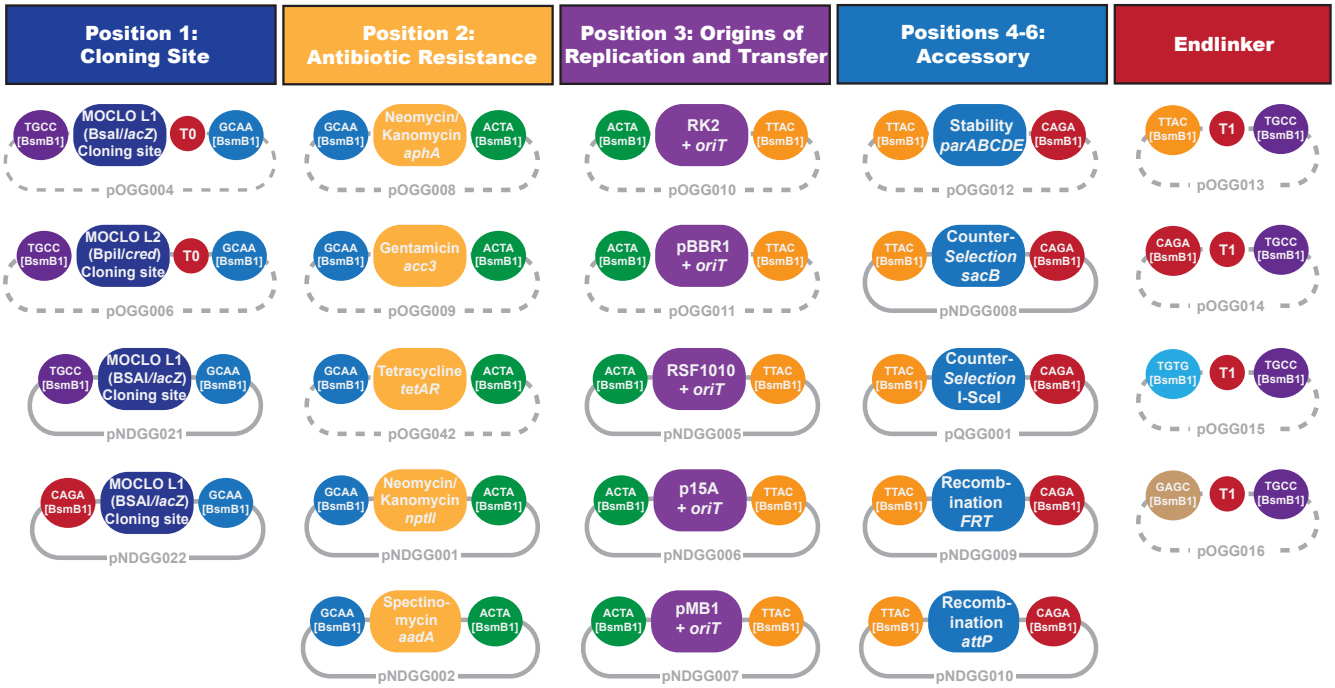

Figure 1. Diagram of vector modules in the expanded BEVA2.0 vector archive. Dashed vector backbones reflect modules from BEVA1.0 (Geddes, Mendoza-Suárez and Poole, 2019). Solid vector backbones reflect BEVA2.0 expansion modules presented in this work. Colored rounded rectangles reflect parts, colored by module type. Colored circles reflect sticky overhangs generated by *BsmB1* and ligated by DNA ligase in Golden Gate cloning reactions.

261 **A suite of broad host range Golden Gate expression vectors**

262 Using the updated BEVA2.0 parts library, we combined several modules with the aim of
263 developing a flexible broad host range vector suite with varied antibiotic resistance. To this end,
264 we included four antibiotic resistance modules (*aadA* (Sp), *nptII* (Nm/Km), *tetAR* (Tc), and *acc3*
265 (Gm); Position 2) with three broad host range origins of replication (RK2, pBBR1 and RSF1010;
266 Position 3). These were combined in the standard BEVA architecture with a Level 1 Golden
267 Gate cloning site (Position 1), the *par* accessary cluster for stability in the absence of antibiotic
268 selection (Position 4), and an endlinker (ELT4). The resulting vectors and their compositions are
269 summarized in **Table 1** and **Figure 2A.**

270 While the *parABCDE* cluster has been characterized for its ability to stabilize RK2
271 plasmids from which it was derived, we wished to verify the compatibility of this module with
272 the heterologous origins of replication pBBR1 and RSF1010. To do so, we performed an
273 experiment to assess plasmid stability in the absence of antibiotic selection, and compared the
274 stability of plasmids that included the module (Lv1-Gm-pBBR1-par-ELT4, and Lv1-Gm-
275 RSF1010-par-ELT4) to vectors we constructed the excluded the *par* module (Lv1-Gm-pBBR1-
276 ELT3, and Lv1-Gm-RSF1010-ELT3). Single colonies of *E. coli* transformants from each
277 plasmid were used to inoculate an overnight culture in the absence of antibiotics. Following
278 overnight growth and saturation, the culture was plated by serial dilution to single colonies
279 without antibiotic selection, and the resulting colonies were patched onto Gm to assess plasmid
280 maintenance. In this experiment, while the pBBR1 vector showed stability in either the presence
281 or absence of *par*, the RSF1010 plasmid was significantly more stable when including the *par*
282 module (**Figure 2B**).

283 To verify Level 1 cloning and suitability of plasmids for expression, one plasmid from
284 each origin of replication from the suite (all Tc^R) were used for Level 1 Golden Gate cloning,
285 wherein we combined sfGFP with a constitutive promoter and ribosome binding site in *E. coli*
286 ST18ALA (**Table 3**). The fluorescence of the resulting plasmids was tested using flow
287 cytometry. We found similar fluorescence profiles in plasmids that contained RK2, pBBR1, or
288 RSF1010 backbones (**Figure 2C**).

289

290

291

292 **Table 1. Plasmids used in this work**

Vector Name	Description	Citation
Vector construction parts used to assemble BEVA2.0 vectors		
pOGG004	BEVA Position 1 Level 1 BsaI cloning site flanked by T0, Sp^R. Addgene 113979	(Geddes, Mendoza-Suárez and Poole, 2019)
pOGG006	BEVA Position 1 Level 2 BpiI cloning site flanked by T0, Sp^R. Addgene 113981	(Geddes, Mendoza-Suárez and Poole, 2019)
pNDGG021	BEVA2.0 Position 1 Level 1 BsaI cloning site without T0, Amp^R	This work
pNDGG022	BEVA2.0 Position 1 Level 1 BsaI cloning site with alternate CAGA 3' fusion site, without T0, Amp^R	This work
pOGG008	BEVA Position 2 Km/Nm antibiotic resistance via *aphA*, $Sp^R/Km^R/Nm^R$. Addgene 113982	(Geddes, Mendoza-Suárez and Poole, 2019)
pOGG009	BEVA Position 2 Gm antibiotic resistance via *aac3*, Sp^R/Gm^R. Addgene 113983	(Geddes, Mendoza-Suárez and Poole, 2019)
pOGG042	BEVA Position 2 Gm antibiotic resistance via *aac3*, Sp^R/Gm^R. Addgene 113998	(Geddes, Mendoza-Suárez and Poole, 2019)
pNDGG001	BEVA2.0 Position 2 Km/Nm antibiotic resistance via *nptII*, $Cm^R/Km^R/Nm^R$.	This work
pNDGG002	BEVA2.0 Position 2 Sp antibiotic resistance via *aadA*, Amp^R/Sp^R	This work
pOGG010	BEVA Position 3 RK2 broad host range origin of replication with *oriT*, Sp^R. Addgene 113984	(Geddes, Mendoza-Suárez and Poole, 2019)
pOGG011	BEVA Position 3 pBBR1 broad host range origin of replication with *oriT*, Sp^R. Addgene 113985	(Geddes, Mendoza-Suárez and Poole, 2019)
pNDGG005	BEVA2.0 Position 3 RSF1010 broad host range origin of replication with *oriT*, Cm^R.	This work
pNDGG006	BEVA2.0 Position 3 p15A narrow host range origin of replication with *oriT*, Cm^R.	This work
pNDGG007	BEVA2.0 Position 3 pMB1 narrow broad host range origin of replication with *oriT*, Cm^R.	This work
pOGG012	BEVA Position 4 *parCDABE* stability locus, Sp^R. Addgene 113986	(Geddes, Mendoza-Suárez and Poole, 2019)
pNDGG008	BEVA2.0 Position 4 *sacB* sucrose counterselection module, Amp^R.	This work
pQGG001	BEVA2.0 Position 4 I-SceI recognition/cut site, Sp^R.	This work
pNDGG009	BEVA2.0 Position 4 *FRT* recombinase site, Amp^R. Also includes *attP* EF module for L1 GG cloning.	This work
pNDGG010	BEVA2.0 Position 4 *attP* recombinase site, Amp^R. Also includes *FRT* EF module for L1 GG cloning.	This work
pOGG013	BEVA Position 3 endlinker with T1 terminator, Sp^R. Addgene 113987	(Geddes, Mendoza-Suárez and Poole, 2019)

pOGG014	BEVA Position 4 endlinker with T1 terminator, Sp^R. Addgene 113988	(Geddes, Mendoza-Suárez and Poole, 2019)
pOGG015	BEVA Position 5 endlinker with T1 terminator, Sp^R. Addgene 113989	(Geddes, Mendoza-Suárez and Poole, 2019)
pOGG016	BEVA Position 6 endlinker with T1 terminator, Sp^R, Addgene 113990	(Geddes, Mendoza-Suárez and Poole, 2019)
BEVA2.0 Vectors used for Level 1 or 2 GG cloning		
pNDGG003	BEVA2.0 Broad host range plasmid with stability. L1-RK2-Tc-par-ELT4; GG assembly from pOGG010, pOGG012, pOGG014, pOGG042, and pOGG004, Tc^R	This work
pNDGG004	BEVA2.0 Broad host range plasmid with stability. L1-pBBR1-Tc-par-ELT4; GG assembly from pOGG011, pOGG012, pOGG014, pOGG042, and pOGG004, Tc^R	This work
pNDGG049	BEVA2.0 Broad host range plasmid with stability. -pBBR1-Gm-par-ELT4; GG assembly from pOGG004, pOGG009, pOGG011, pOGG012, and pOGG014, Gm^R	This work
pNDGG050	BEVA2.0 Broad host range plasmid with stability. L1-RK2-Gm-par-ELT4; GG assembly from pOGG004, pOGG009, pOGG010, pOGG012, and pOGG014, Gm^R	This work
pNDGG051	BEVA2.0 Broad host range plasmid with stability. L1-pBBR1-Sp-par-ELT4; GG assembly from pOGG004, pNDGG002, pOGG011, pOGG012, and pOGG014, Sp^R	This work
pNDGG052	BEVA2.0 Broad host range plasmid with stability. L1-RK2-Sp-par-ELT4; GG assembly from pOGG004, pNDGG002, pOGG010, pOGG012, and pOGG014, Sp^R	This work
pNDGG053	BEVA2.0 Broad host range plasmid with stability. L1-pBBR1-Km-par-ELT4; GG assembly from pOGG004, pNDGG001, pOGG011, pOGG012, and pOGG014, Nm^R/Km^R	This work
pNDGG054	BEVA2.0 Broad host range plasmid with stability. L1-RK2-Km-par-ELT4; GG assembly from pOGG004, pNDGG001, pOGG010, pOGG012, and pOGG014, Nm^R/Km^R	This work
pNDGG056	BEVA2.0 Broad host range plasmid with stability. L1-RSF1010-Gm-par-ELT4; GG assembly from pOGG004, pOGG009, pNDGG005, pOGG012, and pOGG014, Gm^R	This work
pNDGG057	BEVA2.0 Broad host range plasmid with stability. L1-RSF1010-Tc-par-ELT4; GG assembly from pOGG004, pOGG042, pNDGG005, pOGG012, and pOGG014, Tc^R	This work
pNDGG058	BEVA2.0 Broad host range plasmid with stability. L1-RSF1010-Sp-par-ELT4; GG assembly from pOGG004, pNDGG002, pNDGG005, pOGG012, and pOGG014, Sp^R	This work
pNDGG059	BEVA2.0 Broad host range plasmid with stability. L1-RSF1010-Km-par-ELT4; GG assembly from pOGG004, pNDGG001, pNDGG005, pOGG012, and pOGG014, Nm^R/Km^R	This work
pNDGG070	BEVA2.0 Sucrose curable broad host range plasmid . L1-pBBR1-Sp-sacB-ELT4; GG assembly from pOGG004, pNDGG002, pOGG011, pNDGG008, and pOGG014, Sp^R	This work
pQGG002	BEVA2.0 Narrow host range plasmid with I-SceI counterselectable site. L1-P15A-Nm-ISceI; GG assembly from pOGG004, pNDGG001, pNDGG006, pQGG001, pOGG014. Km^R/Nm^R.	This work

pQGG003	BEVA2.0 Narrow host range plasmid with I-SceI counterselectable site for BpiI cloning. L2-P15A-Nm-ISceI; GG assembly from pOGG006, pNDGG001, pNDGG006, pQGG001, pOGG014. $Km^{R/}Nm^{R}$.	This work
pQGG004	BEVA2.0 Narrow host range plasmid with I-SceI counterselectable site. L1-P15A-Gm-ISceI-ELT4; GG assembly from pOGG004, pOGG009, pNDGG006, pQGG001, pOGG014. Gm^{R}.	This work
pQGG005	BEVA2.0 Narrow host range plasmid with I-SceI-ELT4 counterselectable site for BpiI cloning. L2-P15A-Gm-ISceI-ELT4; GG assembly from pOGG006, pOGG009, pNDGG006, pQGG001, pOGG014. Gm^{R}.	This work
pNDGG012	Narrow host range plasmid with *FRT* site. L1-pMB1-Gm-*FRT*-ELT4; GG assembly from pNDGG021, pOGG009, pNDGG007, pNDGG009, pOGG014. Gm^{R}.	This work
pNDGG013	Narrow host range plasmid with *FRT* site. L1-p15A-Km-*FRT*-ELT4; GG assembly from pNDGG021, pOGG009, pNDGG006, pNDGG009, pOGG014. Km^{R}.	This work
pNDGG014	Narrow host range plasmid. L1-pMB1-Gm-ELT3; pNDGG021, pOGG009, pNDGG007, pOGG013. Gm^{R}.	This work
pNDGG015	Narrow host range plasmid. L1-p15A-Km-ELT3; pNDGG021, pOGG009, pNDGG006, pOGG013. Km^{R}.	This work
ORF parts used for BsaI GG cloning		
J23106	CIDAR Medium-strength constitutive promoter from Anderson series, AB module, Amp^{R}, Addgene 65992	(Iverson *et al.*, 2016)
B0032m	CIDAR Weiss RBS of medium strength, BC module, Amp^{R}, Addgene 66020	(Iverson *et al.*, 2016)
BCD12	CIDAR BiCistronic RBS of medium-low strength, BC module, Amp^{R}, Addgene 66023	(Iverson *et al.*, 2016)
C3m	CIDAR MoClo Extension volume I, sfGFP, CD module, Amp^{R}. Addgene 120956	Gift from Richard Murray via Addgene)
C51m	CIDAR MoClo Extension volume I, sfYFP, CD module, Amp^{R}. Addgene 120975	Gift from Richard Murray via Addgene)
C91m	CIDAR MoClo Extension volume I, sfCFP, CD module, Amp^{R}. Addgene 120999	Gift from Richard Murray via Addgene)
C88m	CIDAR MoClo Extension volume I, m-Scarlet-I, CD module, Amp^{R}. Addgene 121003	Gift from Richard Murray via Addgene)
T2m	CIDAR MoClo Extension volume I, Eck120033736 terminator (nmeth.2515), DE module, Amp^{R}. Addgene 121029	Gift from Richard Murray via Addgene)
T12m	CIDAR MoClo Extension volume I, Eck120026300 terminator (nmeth.2515), DE module, Amp^{R}. Addgene 121031	Gift from Richard Murray via Addgene)
T15m	CIDAR MoClo Extension volume I, L3S3P11 terminator (nmeth.2515), DE module, Amp^{R}. Addgene 121034	Gift from Richard Murray via Addgene)
pOGG037	BEVA1.0 sfGFP "PU" model (CE CIDAR extensions), Sp^{R}. Addgene 113995	(Geddes, Mendoza-Suárez and Poole, 2019)
pNDGG037	BEVA2.0 T2m terminator with DF extension for CIDAR MoClo Golden Gate Assembly, DF module. Cloned via BpiI GG Assembly of PCR amplicon into POGG006, Sp^{R}.	This work

pNDGG038	BEVA2.0 T12m terminator with DF extension for CIDAR MoClo Golden Gate Assembly, DF module. Cloned via BpiI GG Assembly of PCR amplicon into POGG006, Sp^R.	This work
pNDGG039	BEVA2.0 T15m terminator with DF extension for CIDAR MoClo Golden Gate Assembly, DF module. Cloned via *BpiI* GG Assembly of PCR amplicon into POGG006, Sp^R.	This work
Other plasmids		
pDA1-SceI-sacB	pBBR1 broad host range plasmid expressing I-SceI homing endonuclease and *sacB* counterselectable marker, Tc^R	(Aubert, Hamad and Valvano, 2014)
pNDMS450	RK2 broad host range plasmid expressing constitutive sfGFP. GG assembly of pNDGG054_AF, J23106_AB, B0032m_BC, pOGG037_CE, and EF oligo , Tc^R	This work
pNDMS451	pBBR1 broad host range plasmid expressing constitutive sfGFP. GG assembly of pNDGG053_AF, J23106_AB, B0032m_BC, pOGG037_CE, and EF oligo , Tc^R	This work
pNDMS459	RSF1010 broad host range plasmid expressing constitutive sfGFP. GG assembly of pNDGG054_AF, J23106_AB, B0032m_BC, pOGG037_CE, and EF oligo , Tc^R	This work
pNDMS054	RK2 broad host range plasmid expressing constitutive sfGFP. GG assembly from pNDGG003_AF, J23106_AB, BCD12_BC, C3m_CD, and T2m_DF (pNDGG037), Tc^R	This work
pNDMS055	RK2 broad host range plasmid expressing constitutive sfCFP. GG assembly from pNDGG003_AF, J23106_AB, BCD12_BC, C91m_CD, and T2m_DF (pNDGG037), Tc^R	This work
pNDMS056	RK2 broad host range plasmid expressing constitutive sfYFP. GG assembly from pNDGG003, J23106_AB, BCD12_BC, C51m_CD, and T2m_DF (pNDGG037), Tc^R	This work
pNDMS057	RK2 broad host range plasmid expressing constitutive m-Scarlet-I. GG assembly from pNDGG003, J23106_AB, BCD12_BC, C99m_CD, and T2m_DF (pNDGG037), Tc^R	This work

We also demonstrated the flexibility of the BEVA system by cloning an alternate broad host range plasmid that included a module to facilitate its removal rather than promote stability, *sacB* (Figure 2B). We used a plasmid (Lv1-Sp-pBBR1-sacB-ELT4) to facilitate curing (i.e., loss) of the difficult to remove pBBR1 plasmids from strains of a *S. meliloti* deletion library (Milunovic *et al.*, 2014) through incompatibility. Thereafter, we found that the BEVA2.0 *sacB* plasmid was efficiently removed by sucrose counterselection (**Figure 2E**). In four replicates, *S. meliloti* bearing the Sp^R *sacB* plasmid were plated onto LBmc or LBmc with 10% sucrose by serial dilution following overnight culturing in the absence of antibiotics. Approximately 50 single colonies from each set of plates were patched onto LBmc Sp to test for plasmid loss. A low rate of plasmid loss was observed in the absence of sucrose selection, while sucrose selection resulted in a complete curing of the plasmid in the population tested.

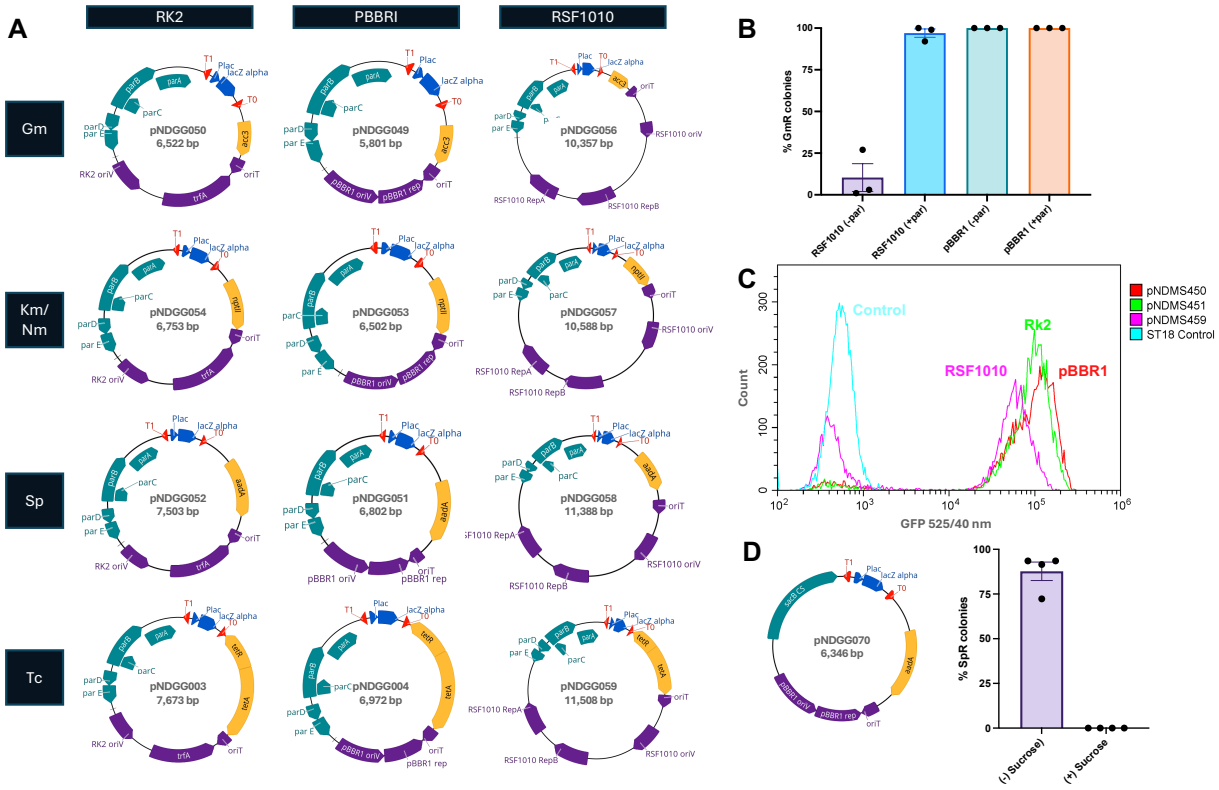

Figure 2. BEVA2.0 Broad Host Range Vectors. A. Plasmid maps of broad host range vectors developed using BEVA2.0 parts. Nucleotide sequences of the plasmids are included in the supplemental data. **B.** Quantification of pBBR1 or RSF1010 plasmid maintenance with and without *par* loci. Data is expressed as the proportion of colonies that grew on LB + Gm plates after patching following antibiotic-free culturing and spread-plating on LB. **C.** Histograms of GFP signal from flow cytometry analysis of *E. coli* ST18ALA bearing RSF1010, pBBR1, or RK2 plasmids expressing sfGFP. **D.** Plasmid map of a curable *sacB*-containing pBBR1 plasmid pNDGG070, and the proportion of plasmid loss following growth on 10% sucrose based on sensitivity when colonies were patched on LB + Sp media.

Golden-Gate compatible vectors for homologous recombination

We also expanded the collection of Level 1 cloning vectors for use in genetic engineering by utilizing integrative plasmid parts from the updated BEVA2.0 parts library (Table 1). Vectors for homologous recombination were constructed using the p15A origin of replication, which generates integrative plasmids in many Gram-negative bacteria due to its inability to be

322 maintained as a replicating plasmid (Quandt and Hynes, 1993) (Figure 3A). To facilitate
323 workflows for constructing deletions by double homologous recombination, we also added an I-
324 SceI recognition site that enables curing through expression of the I-*SceI* endonuclease. We
325 generated multiple versions including optional antibiotic selection (Gm^R or Nm^R), and two
326 different cloning sites (BsaI or BpiI) to facilitate flexible cloning of chromosomal homologous
327 regions, should one site or the other be present in a target region. These plasmids have been used
328 in workflows to generate deletions in *S. meliloti* and functioned efficiently to generate marked or
329 unmarked deletions. For example, when a pQGG004 derivative was used to create a marked
330 deletion of the *S. meliloti phaZ* gene, the efficiency of I-SceI selection for the expected double-
331 recombination was ~14% when averaged across four independent replicates with 17-33 colonies.
332 Surprisingly, the efficiency varied from as low as 3% to up to 19% depending on the trial, which
333 is a result that we have repeatedly observed when selecting for double recombinants using this
334 approach (diCenzo, unpublished). We hypothesize that the efficiency of obtaining double
335 recombinants varies depending on where the initial recombination occurred, and thus we
336 recommend purifying multiple single recombinants for use in downstream steps to optimize the
337 likelihood of obtaining a correct double recombinant.

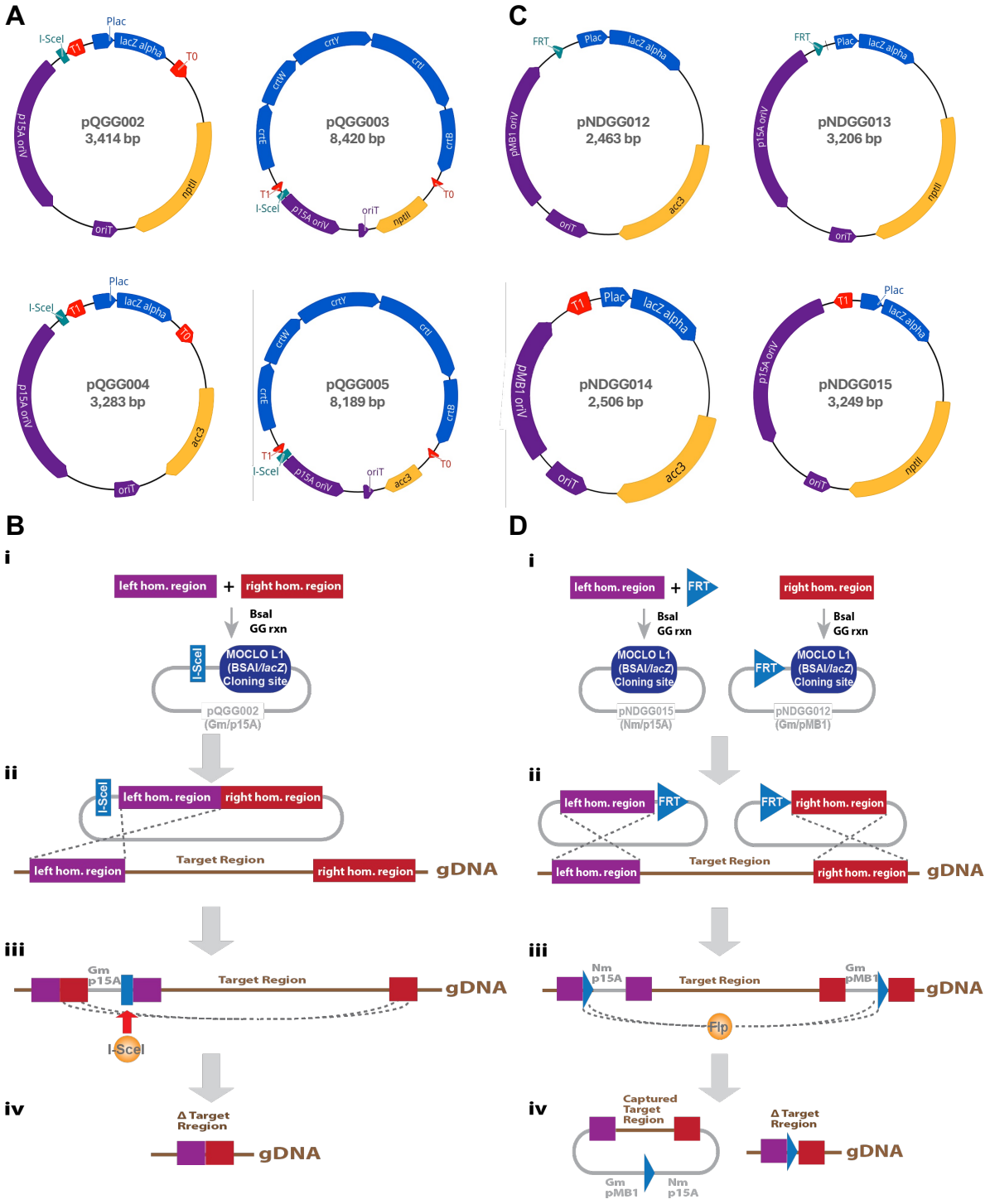

Figure 3. BEVA2.0 Genome Manipulation Plasmids. A. Maps of plasmids developed for the double homologous recombination deletion method, and **B.** schematic of the use of the plasmids to delete a target region. Steps involve: **i)** cloning of homologous regions to the left and right of

342 the target region into a BEVA2.0 vector using BsaI or BpiI Golden Gate cloning; **ii)** conjugating
343 the plasmid into the target organism and selecting for integration via single cross-over
344 homologous recombination (using antibiotic resistance on the plasmid); **iii)** introducing a
345 replicating plasmid expressing the I-SceI endonuclease (eg. via pDA1-ISceI-sacB) by
346 conjugation and selecting for its maintenance to select for the second recombination event, in
347 which the BEVA2.0 plasmid backbone is excised from the genome together with the target
348 region; and **iv)** screening resulting colonies for the presence of the deletion (based on PCR and
349 loss of the resistance of the BEVA2.0 plasmid). **C.** Maps of plasmids developed for Flp/*FRT*
350 recombination methods, and **D.** a schematic diagramming their use to excise and capture a target
351 region. Steps involve: **i)** cloning homologous regions to the left and right of the target adjacent to
352 *FRT* site in heterologous BEVA2.0 plasmids via BsaI Golden Gate cloning; **ii)** sequentially
353 integrating the plasmids by conjugating them into the recipient and selecting for the appropriate
354 antibiotic resistances; **iii)** introducing a replicating plasmid containing *flp* recombinase gene (eg.
355 pTH2505) by conjugation and inducing Flp expression to catalyze excision of the target region
356 via *FRT* recombination (optionally also introducing an *E. coli* recipient strain for region capture,
357 and selecting with an alternate media that selects for the recipient with BEVA2.0 plasmids); and
358 **iv)** screening for the resulting deletion by PCR and loss of BEVA2.0 backbone resistance.
359

360 **Adapting the Flp/*FRT* deletion method to Golden Gate plasmid assembly**

361 Another workflow for genetic manipulation involves the use of site-specific recombinases such
362 as FLP, ϕC31, or Cre to generate deletions, inversions, or integrations (diCenzo and Finan,
363 2018). We have found these particularly useful for deleting or integrating large regions
364 (Milunovic *et al.*, 2014; Geddes *et al.*, 2021). To adapt these workflows to Golden Gate cloning,
365 we generated additional new integrative vectors. Since deletion workflows require sequential
366 integration of recombinase sites flanking either side of a target, it is valuable to have a second
367 heterologous integrative plasmid (diCenzo and Finan, 2018). It is optimal to minimize homology
368 between the two plasmids, therefore in addition to p15A-based plasmids, we also generated
369 integrative plasmids based on another integrative origin of replication, pMB1 and excluded the
370 terminators that flank the cloning site in the BEVA architecture. We used an alternate Level 1
371 Golden Gate cloning site (vector pNDGG0022) that excluded the 3' T_0 terminator, and replaced
372 the endlinker T1 terminator with an *FRT* site (vector pNDGG009). We designed a scheme

373 wherein a *FRT* site can be incorporated into the 5' end of a cloned homologous region from the
374 genome by using the *FRT*-bearing vectors, or to the 3' end of a cloned homologous region during
375 region addition. To facilitate addition of the second *FRT* site, we generated an *FRT* site flanked
376 by BsaI and 5' GCTT and 3' CGCT junctions (Figure 3C). We utilized these plasmids to
377 construct an *idhA* deletion in *S. meliloti* RmP110 (Geddes, unpublished) and found them to
378 function with similar efficiencies to traditional cloning plasmids (diCenzo and Finan, 2018).
379

380 **Linking the CIDAR parts archive to BEVA plasmids.**

381 The recently introduced CIDAR MoClo parts kit and CIDAR MoClo Expansion Volume I
382 libraries (available as Kit 1000000059 and Kit 1000000161 through Addgene) include a wide
383 variety of useful parts for bacterial engineering domesticated as defined parts for Level 1 Golden
384 Gate cloning. Because both systems (CIDAR and BEVA) adopt MoClo (Weber *et al.*, 2011),
385 both systems adopt the same fusion sites for Level 1 cloning and, as such, the systems are
386 generally compatible. However, individual CIDAR Level 0 parts were developed with an
387 alternate Positional architecture than BEVA or MoClo (Weber *et al.*, 2011; Iverson *et al.*, 2016;
388 Geddes, Mendoza-Suárez and Poole, 2019) (**Figure 4A-C**). In particular, while the 5' fusion site
389 GGAG ("A" in CIDAR) is conserved between the two systems and links to the 5' fusion site of
390 promoter parts, the 3' cloning fusion site in BEVA is CGCT ("F" in CIDAR), whereas CIDAR
391 was designed with terminators bearing a 3' fusion site of GCTT ("E"). Therefore, to adapt
392 BEVA to the CIDAR architecture, we recloned several CIDAR terminators to match the 3'
393 fusion site of BEVA plasmids (as "DF" rather than "DE" parts). Using these terminators enables
394 researchers to utilize the wide variety of CIDAR parts for construction of open reading frames in
395 BEVA plasmids. For example, we have cloned a variety of constitutively expressed fluorescent
396 proteins by combining promoters, RBS, and open reading frames from CIDAR into the
397 replicating plasmid pNDGG003 and verified their function in *S. meliloti* (**Figure 4E-H**, **Table**
398 **1**).

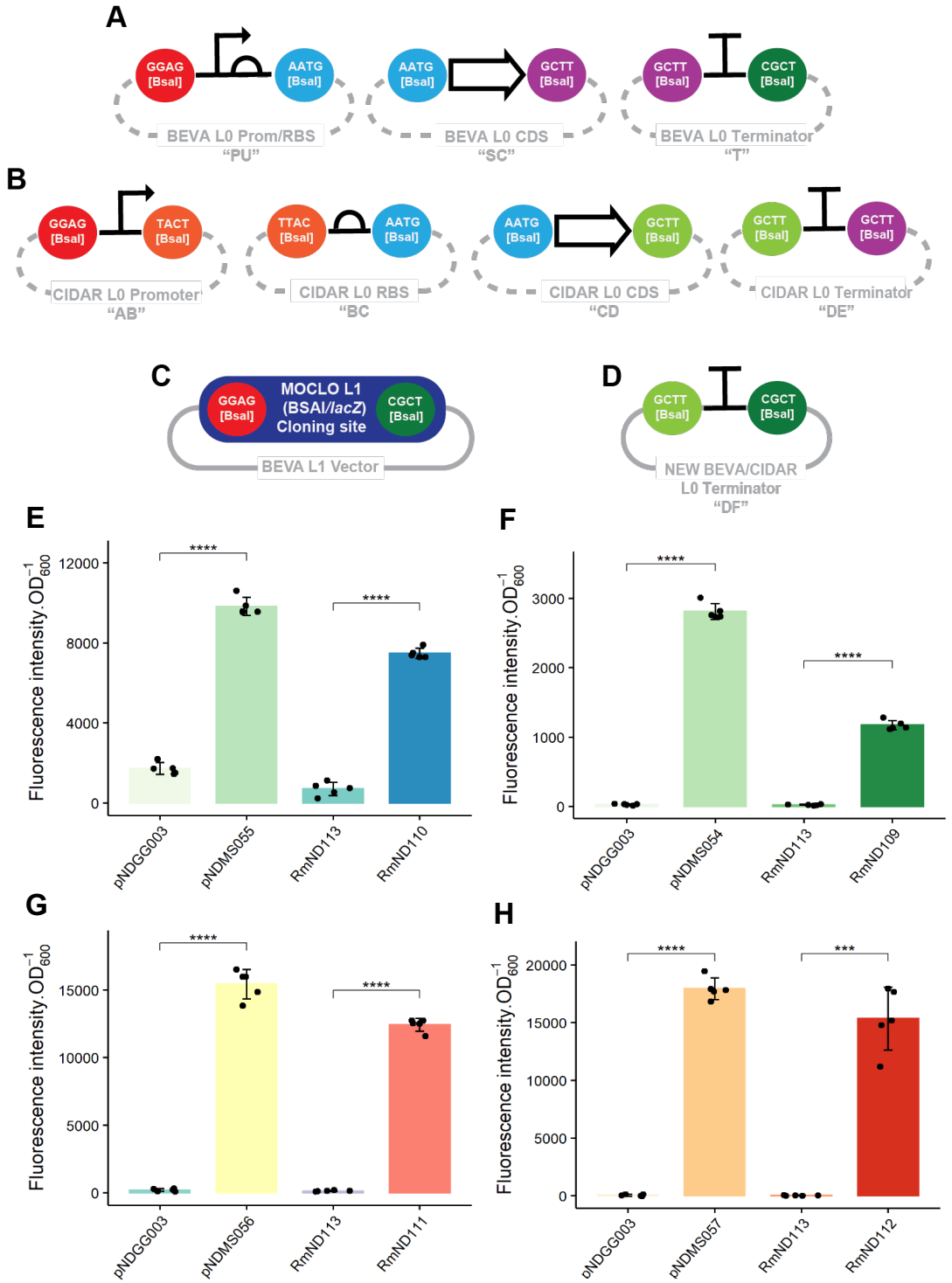

Figure 4. Parts to link BEVA and CIDAR. A. Diagram of the architecture of BEVA Level 0 parts for open reading frame construction (Geddes, Mendoza-Suárez and Poole, 2019). **B.** Diagram of the architecture of CIDAR parts for open reading frame construction.

403 **C.** Architecture of a the BsaI multiple cloning site in Level 1 BEVA vectors. **D.** Architecture of
404 BEVA/SEVA "linker" DF terminators. **E.** Fluorescence of BEVA vectors with CIDAR parts.
405 The constitutive promoter J23106 together with the medium-strength RBS BCS12, are used to
406 drive sfCFP (E), sfGFP (F), sfYFP (G) and mScarlet-I (H). The new linker terminator was used
407 to assemble these marker genes in the RK2 BEVA2.0 plasmid pNDGG003. Fluorescence of the
408 cloned plasmids in *E. coli* (pNDMS054-57) is shown next to the empty vector control
409 (pNDGG003) on the left side of the graphs. On the right side of the graphs, *S. meliloti* RmP110
410 containing pNDGG003 (RmND113) is shown compared to RmP110 containing pNDMS054-57
411 (RmND109-112).
412
413 **Conclusions**
414 The original Bacterial Expression Vector Archive has facilitated new synthetic biology
415 approaches for alpha-proteobacteria such as advanced strain barcoding (Mendoza-Suárez *et al.*,
416 2020) and adaption of CRISPR base editing (Wang *et al.*, 2021), and has supported a range of
417 studies by streamlining genetic engineering (Geddes *et al.*, 2019; Haskett *et al.*, 2022, 2023). In
418 addition, adaptations of the BEVA architecture have recently been performed for the
419 development of a suite of plasmids for Tn*7* (Jorrin *et al.*, 2024) and mariner transposition
420 (Williamson et al. in Preparation). The resources presented here in the BEVA2.0 expansion will
421 further expand the utility of the system by extending the host range of replicating plasmids with
422 new origins of replication and antibiotic resistance modules, introducing resources for genetic
423 engineering by homologous or site-specific recombination, and adapting BEVA plasmids to
424 function with the CIDAR system. Overall, BEVA and BEVA2.0 represent a significant
425 community resource for bacterial genetics and synthetic biology.
426
427 **Acknowledgements**
428 This work was supported by a New Innovator in Food & Agricultural Research (FFAR) grant to
429 B. A. Geddes ID: FF-NIA21-0000000061m, an NSF Collaborative Research-PGR grant to B. A.
430 Geddes: Award number 2243818. Research in the G.C.D. laboratory is supported by the Natural
431 Sciences and Engineering Research Council of Canada (NSERC) through the Discovery Grants
432 program (grant number RGPIN-2020-07000).
433

434 **Data Availability**

435 Golden Gate cloning plasmids generated in this work and their DNA sequence information have
436 been submitted to Addgene (Deposit 85226). Data supporting figures in the manuscript is
437 available upon request.

438

439 **Competing Interests**

440 Barney A. Geddes and Riley Williamson are co-founders of Frontier Bioforge LLC. Barney A.
441 Geddes is a co-founder of Lilac Agriculture Inc.

442

443 **References**

444 Aubert, D.F., Hamad, M.A. and Valvano, M.A. (2014) 'A markerless deletion method for
445 genetic manipulation of Burkholderia cenocepacia and other multidrug-resistant gram-negative
446 bacteria', *Methods in Molecular Biology (Clifton, N.J.)*, 1197, pp. 311–327. Available at:
447 https://doi.org/10.1007/978-1-4939-1261-2_18.

448 Bentham, A.R. *et al.* (2021) 'pOPIN-GG: A resource for modular assembly in protein expression
449 vectors'. bioRxiv, p. 2021.08.10.455798. Available at:
450 https://doi.org/10.1101/2021.08.10.455798.

451 diCenzo, G.C. *et al.* (2019) 'Multidisciplinary approaches for studying rhizobium–legume
452 symbioses', *Canadian Journal of Microbiology*, 65(1), pp. 1–33. Available at:
453 https://doi.org/10.1139/cjm-2018-0377.

454 diCenzo, G.C. and Finan, T.M. (2018) 'Techniques for large-scale bacterial genome
455 manipulation and characterization of the mutants with respect to in silico metabolic
456 reconstructions', in M. Fondi (ed.) *Metabolic Network Reconstruction and Modeling: Methods*
457 *and Protocols*. New York, NY: Springer, pp. 291–314. Available at: https://doi.org/10.1007/978-
458 1-4939-7528-0_13.

459 Engler, C. *et al.* (2009) 'Golden Gate Shuffling: A One-Pot DNA Shuffling Method Based on
460 Type IIs Restriction Enzymes', *PLoS ONE*, 4(5), p. e5553. Available at:
461 https://doi.org/10.1371/journal.pone.0005553.

462 Engler, C. *et al.* (2014) 'A Golden Gate Modular Cloning Toolbox for Plants', *ACS Synthetic*
463 *Biology*, 3(11), pp. 839–843. Available at: https://doi.org/10.1021/sb4001504.

464 Finan, T.M. *et al.* (1986) 'Second symbiotic megaplasmid in *Rhizobium meliloti* carrying
465 exopolysaccharide and thiamine synthesis genes', *Journal of Bacteriology*, 167(1), pp. 66–72.
466 Available at: https://doi.org/10.1128/jb.167.1.66-72.1986.

467 Gantner, J. *et al.* (2018) 'Peripheral infrastructure vectors and an extended set of plant parts for
468 the Modular Cloning system', *PloS One*, 13(5), p. e0197185. Available at:
469 https://doi.org/10.1371/journal.pone.0197185.

470 Geddes, B.A. *et al.* (2019) 'Engineering transkingdom signalling in plants to control gene
471 expression in rhizosphere bacteria', *Nature communications*, 10(1), pp. 1–11. Available at:
472 https://doi.org/10.1038/s41467-019-10882-x.

473 Geddes, B.A. *et al.* (2021) 'Minimal gene set from *Sinorhizobium* (*Ensifer*) *meliloti* pSymA
474 required for efficient symbiosis with *Medicago*', *Proceedings of the National Academy of*
475 *Sciences*, 118(2). Available at: https://doi.org/10.1073/pnas.201801511.

476 Geddes, B.A., Mendoza-Suárez, M.A. and Poole, P.S. (2019) 'A bacterial expression vector
477 archive (BEVA) for flexible modular assembly of Golden Gate-compatible vectors', *Frontiers in*
478 *Microbiology*, 9, p. 3345. Available at: https://doi.org/10.3389/fmicb.2018.03345.

479 Grützner, R. *et al.* (2021) 'High-efficiency genome editing in plants mediated by a Cas9 gene
480 containing multiple introns', *Plant Communications*, 2(2), p. 100135. Available at:
481 https://doi.org/10.1016/j.xplc.2020.100135.

482 Hahn, F. *et al.* (2020) 'A modular cloning toolkit for genome editing in plants', *BMC plant*
483 *biology*, 20(1), p. 179. Available at: https://doi.org/10.1186/s12870-020-02388-2.

484 Haskett, T.L. *et al.* (2022) 'Control of nitrogen fixation and ammonia excretion in *Azorhizobium*
485 *Caulinodans*', *PLOS Genetics*, 18(6), p. e1010276. Available at:
486 https://doi.org/10.1371/journal.pgen.1010276.

487 Haskett, T.L. *et al.* (2023) 'Rhizopine biosensors for plant-dependent control of bacterial gene
488 expression', *Environmental Microbiology*, 25(2), pp. 383–396. Available at:
489 https://doi.org/10.1111/1462-2920.16288.

490 Iverson, S.V. *et al.* (2016) 'CIDAR MoClo: Improved MoClo assembly standard and new *E. coli*
491 part library enable rapid combinatorial design for synthetic and traditional biology', *ACS*
492 *Synthetic Biology*, 5(1), pp. 99–103. Available at: https://doi.org/10.1021/acssynbio.5b00124.

493 Jorrin, B. *et al.* (2024) 'Stable, fluorescent markers for tracking synthetic communities and
494 assembly dynamics', *Microbiome*, 12(1), p. 81. Available at: https://doi.org/10.1186/s40168-
495 024-01792-2.

496 Lee, H.H. *et al.* (2019) 'Functional genomics of the rapidly replicating bacterium Vibrio
497 natriegens by CRISPRi', *Nature Microbiology*, 4(7), pp. 1105–1113. Available at:
498 https://doi.org/10.1038/s41564-019-0423-8.

499 Lee, M.E. *et al.* (2015) 'A Highly Characterized Yeast Toolkit for Modular, Multipart
500 Assembly', *ACS Synthetic Biology*, 4(9), pp. 975–986. Available at:
501 https://doi.org/10.1021/sb500366v.

Martínez-García, E. *et al.* (2023) 'SEVA 4.0: an update of the Standard European Vector Architecture database for advanced analysis and programming of bacterial phenotypes', *Nucleic Acids Research*, 51(D1), pp. D1558–D1567. Available at: https://doi.org/10.1093/nar/gkac1059.

Mendoza-Suárez, M.A. *et al.* (2020) 'Optimizing Rhizobium-legume symbioses by simultaneous measurement of rhizobial competitiveness and N2 fixation in nodules', *Proceedings of the National Academy of Sciences*, 117(18), pp. 9822–9831. Available at: https://doi.org/10.1073/pnas.1921225117.

Milunovic, B. *et al.* (2014) 'Cell growth inhibition upon deletion of four toxin-antitoxin loci from the megaplasmids of *Sinorhizobium meliloti*', *Journal of Bacteriology*, 196(4), pp. 811–824. Available at: https://doi.org/10.1128/JB.01104-13.

Moore, S.J. *et al.* (2016) 'EcoFlex: A multifunctional MoClo Kit for *E. coli* synthetic biology', *ACS Synthetic Biology*, 5(10), pp. 1059–1069. Available at: https://doi.org/10.1021/acssynbio.6b00031.

Obst, U., Lu, T.K. and Sieber, V. (2017) 'A modular toolkit for generating *Pichia pastoris* secretion libraries', *ACS Synthetic Biology*, 6(6), pp. 1016–1025. Available at: https://doi.org/10.1021/acssynbio.6b00337.

Prentki, P. and Krisch, H.M. (1984) 'In vitro insertional mutagenesis with a selectable DNA fragment', *Gene*, 29(3), pp. 303–313. Available at: https://doi.org/10.1016/0378-1119(84)90059-3.

Quandt, J. and Hynes, M.F. (1993) 'Versatile suicide vectors which allow direct selection for gene replacement in gram-negative bacteria', *Gene*, 127(1), pp. 15–21. Available at: https://doi.org/10.1016/0378-1119(93)90611-6.

Schweizer, H.P. and Hoang, T. (1996) 'Improved methods for gene analysis and expression in Pseudomonas'.

Silva-Rocha, R. *et al.* (2013) 'The Standard European Vector Architecture (SEVA): a coherent platform for the analysis and deployment of complex prokaryotic phenotypes', *Nucleic Acids Research*, 41(Database issue), pp. D666–D675. Available at: https://doi.org/10.1093/nar/gks1119.

Stuttmann, J. *et al.* (2021) 'Highly efficient multiplex editing: one-shot generation of 8× Nicotiana benthamiana and 12× Arabidopsis mutants', *The Plant Journal: For Cell and Molecular Biology*, 106(1), pp. 8–22. Available at: https://doi.org/10.1111/tpj.15197.

Wang, L. *et al.* (2021) 'Highly Efficient CRISPR-Mediated Base Editing in Sinorhizobium meliloti', *Frontiers in Microbiology*, 12. Available at: https://doi.org/10.3389/fmicb.2021.686008.

Weber, E. *et al.* (2011) 'A modular cloning system for standardized assembly of multigene constructs', *PloS One*, 6(2), p. e16765. Available at: https://doi.org/10.1371/journal.pone.0016765.

539 Werner, S. *et al.* (2012) 'Fast track assembly of multigene constructs using Golden Gate cloning
540 and the MoClo system', *Bioengineered Bugs*, 3(1), pp. 38–43. Available at:
541 https://doi.org/10.4161/bbug.3.1.18223.

542